View metadata, citation and similar papers at core.ac.uk

brought to you by CORE

provided by Elsevier - Publisher Connector

Partitioning of Individual Flexible Polymers into a Nanoscopic Protein Pore

Liviu Movileanu,* Stephen Cheley,* and Hagan Bayley*†

*Department of Medical Biochemistry and Genetics, The Texas A&M University System Health Science Center, College Station, Texas; and †Department of Chemistry, Texas A&M University, College Station, Texas

ABSTRACT Polymer dynamics are of fundamental importance in materials science, biotechnology, and medicine. However, very little is known about the kinetics of partitioning of flexible polymer molecules into pores of nanometer dimensions. We employed electrical recording to probe the partitioning of single poly(ethylene glycol) (PEG) molecules, at concentrations near the dilute regime, into the transmembrane β-barrel of individual protein pores formed from staphylococcal α-hemolysin (αHL). The interactions of the α-hemolysin pore with the PEGs (M_w 940–6000 Da) fell into two classes: short-duration events ($\tau \sim 20$ μs), ~85% of the total, and long-duration events ($\tau \sim 100$ μs), ~15% of the total. The association rate constants (k_{on}) for both classes of events were strongly dependent on polymer mass, and values of k_{on} ranged over two orders of magnitude. By contrast, the dissociation rate constants (k_{off}) exhibited a weak dependence on mass, suggesting that the polymer chains are largely compacted before they enter the pore, and do not decompact to a significant extent before they exit. The values of k_{on} and k_{off} were used to determine partition coefficients (Π) for the PEGs between the bulk aqueous phase and the pore lumen. The low values of Π are in keeping with a negligible interaction between the PEG chains and the interior surface of the pore, which is independent of ionic strength. For the long events, values of Π decrease exponentially with polymer mass, according to the scaling law of Daoud and de Gennes. For PEG molecules larger than ~5 kDa, Π reached a limiting value suggesting that these PEG chains cannot fit entirely into the β-barrel.

INTRODUCTION

The interaction of polymer molecules with proteinaceous pores is of fundamental importance both in basic science and in biotechnology. In basic science, polymers have been used to investigate the size and shape of protein pores (Vodyanoy and Bezrukov, 1992; Krasilnikov et al., 1992; Carneiro et al., 1997; Merzlyak et al., 1999; Movileanu and Bayley, 2001). The transport of polymers through pores is also of considerable physiological importance (Bläsi and Young, 1996; Johnson and van Waes, 1999; Gomis-Rüth et al., 2001; Madden et al., 2001; Salman et al., 2001), but few fundamental studies of the mechanism of this process have been made. Work with protein pores also provides an opportunity to investigate polymer dynamics and the properties of confined polymers, which have been subjected to theoretical inquiry (Sung and Park, 1996; Lubensky and Nelson, 1999; de Gennes, 1999a; Muthukumar, 1999; Cifra and Bleha, 2001; Berezhkovskii and Gopich, 2003) but more limited experimentation (Wong et al., 1997; Smith et al., 1999; LeDuc et al., 1999; Jeppesen et al., 2001). Technological applications of polymer-pore interactions include gel permeation chromatography (Gorbunov and Skvortsov, 1995; Liu et al., 1999) and the use of protein pores as components of biosensors (Bayley et al., 2000; Bayley and Cremer, 2001; Wang and Branton, 2001).

The interactions of poly(ethylene glycol) (PEG) have been examined with several protein pores (Parsegian et al., 1995; Bezrukov, 2000). Early work included investigation of the osmotic effects of PEG on the opening and closing of the voltage-dependent anion channel of mitochondria (Zimmerberg and Parsegian, 1986). The effects of PEG on the access resistance of pores such as those formed by alamethicin were also examined (Vodyanoy and Bezrukov, 1992, 1993). Especially relevant to the present work, single-channel conductance and single-channel noise measurements were used to deduce the dependence of the partitioning of PEG molecules into the alamethicin pore on PEG mass, and the diffusion coefficients of the PEG molecules within the pore (Bezrukov and Vodyanoy, 1993, 1995; Bezrukov et al., 1994).

A particularly useful subject for studies with polymers has been the bacterial exotoxin α-hemolysin (αHL), which forms large pores in lipid bilayers (Song et al., 1996; Gouaux, 1998). The pore is formed from seven identical subunits, each containing 293 amino acids, and its three-dimensional structure is known (Song et al., 1996). The transmembrane part of the pore, which is exposed to the *trans* side of the bilayer, is a β-barrel of ~20-Å average diameter and ~50-Å length. The cap domain, which lies on the *cis* side of the bilayer, contains a large internal cavity (Fig. 1). Bezrukov and colleagues have investigated the interactions of PEG with αHL in detail. In their work, which was performed at high PEG concentrations, the partition coefficient for the transfer of PEG from bulk solution to the interior of the pore had a sharp dependence on PEG mass, which is not consistent with scaling theory (see below). Further, single-channel current fluctuations in the presence of PEG

Submitted July 23, 2002, and accepted for publication April 1, 2003.

Address reprint requests to Hagan Bayley, PhD, Dept. of Medical Biochemistry and Genetics, The Texas A&M University System Health Science Ctr., 440 Reynolds Medical Bldg., College Station, TX 77843-1114. Tel.: 979-845-7047; Fax: 979-847-9481; E-mail: bayley@tamu.edu.

© 2003 by the Biophysical Society

0006-3495/03/08/897/14 $2.00

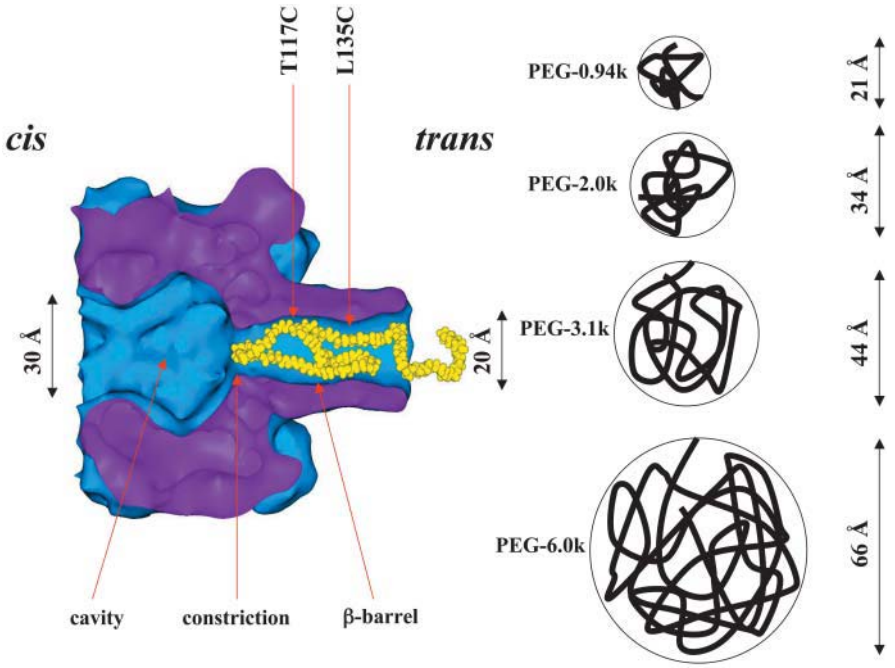

FIGURE 1 Model of the αHL pore and relative sizes of the PEG polymers. The section through the αHL pore shows a PEG molecule of 2.0 kDa inside the transmembrane β-barrel. The sites where replacements with cysteine were made are shown (Thr-117 and Leu-135). The Flory radii of four of the PEG molecules used here are shown.

suggested that PEG binds to the wall of the lumen of the pore in 1 M KCl (Bezrukov et al., 1996). It was also shown that at low pH the size of PEG molecules that enter the pore is decreased, whereas the conductance of the pore is increased; this finding was attributed to the effect of protein charge on water structure and hence the extent of polymer hydration inside the pore (Bezrukov and Kasianowicz, 1997). Finally, the interaction of PEG was reexamined with one-sided application. The effects of *cis* and *trans* additions were different and permitted a more detailed analysis of pore geometry than had been possible by two-sided addition (Merzlyak et al., 1999). In these experiments, the buffer contained 0.1 M KCl and it was concluded that there was no interaction of PEG with the lumen of the pore at this salt concentration.

The interactions of single-stranded nucleic acids with the αHL pore have also been studied in detail. Following the initial report of Kasianowicz and colleagues, demonstrating the transit of nucleic acids through the pore at $\sim$1–5 μs/base (Kasianowicz et al., 1996), a surge of articles has appeared in which several aspects of the phenomenon have been examined including the characteristic current signatures of polynucleotides of different compositions, the impact of *cis* or *trans* entry with respect to the rate of occurrence of transit events, the voltage and temperature dependencies of transit, and the effect of ligands for derivatized DNAs or intramolecular hairpins on transit (Akeson et al., 1999; Henrickson et al., 2000; Meller et al., 2000, 2001; Kasianowicz et al., 2001; Vercoutere et al., 2001, 2003; Meller and Branton, 2002; Winters-Hilt et al., 2003). The work is intriguing because it has been suggested that it may lead to techniques for ultrarapid DNA sequencing (Deamer and Akeson, 2000; Marziali and Akeson, 2001; Vercoutere and Akeson, 2002; Deamer and Branton, 2002). The experiments with polynucleotides have prompted a large number of theoretical treatments of the associated phenomena (Lubensky and Nelson, 1999; de Gennes, 1999a,b; Muthukumar, 1999, 2001, 2002; Nakane et al., 2002; Slater et al., 2002; Kong and Muthukumar, 2002; Ambjornsson et al., 2002; Berezhkovskii and Gopich, 2003).

Our group has also examined the interactions of polymers with the αHL pore, but under very different conditions. In particular, we have focused on the covalent attachment of polymers (Howorka et al., 2000). A qualitative analysis of the rates of reaction of sulfhydryl-directed PEG reagents with a collection of pores assembled from cysteine mutants of αHL was consistent with the position of a constriction in the lumen of the pore (Movileanu et al., 2001). By contrast with the results obtained by Bezrukov and colleagues, quantitative analysis of the chemical modification data revealed that, when low concentrations of the reagents are used, they have little interaction with the wall of the lumen and partition into the pore according to the scaling law of Daoud and de Gennes (1977; Movileanu and Bayley, 2001). In additional work, with covalently attached polymers, we have examined the capture of proteins by biotin at the end of a long PEG chain (Movileanu et al., 2000) and duplex formation with tethered oligonucleotides (Howorka et al., 2001a,b; Howorka and Bayley, 2002). These experiments again revealed details of the properties of polymers, notably their motion within the pore.

In the present work, we set out to reconcile the results obtained from studies with free PEG at high concentrations and chemical modification with sulfhydryl-directed PEGs, by examining the interaction of dilute free polymers with the

αHL pore by using single-channel recording at high time resolution.

MATERIALS AND METHODS

Polyethylene glycols

Polyethylene glycols were purchased and used without further purification. The number-average (M_n) and weight-average (M_w) molecular masses of the reagents were determined by gel permeation chromatography by the manufacturers. The ratio M_w/M_n is directly related to the variance of the mass distribution of a polymer (Strobl, 1997). We used the following reagents: PEG-0.94 k ($M_w = 940$, $M_w/M_n = 1.05$), PEG-2.0 k ($M_w = 1960$, $M_w/M_n = 1.03$), PEG-3.1 k ($M_w = 3060$, $M_w/M_n = 1.03$), PEG-4.2 k ($M_w = 4240$, $M_w/M_n = 1.03$), PEG-6.0 k ($M_w = 6000$, $M_w/M_n = 1.03$) from Fluka (St Louis, MO). We also used PEG-0.30 k ($M_w = 296$, $M_w/M_n = 1.05$), PEG-0.40 k ($M_w = 404$, $M_w/M_n = 1.05$), PEG-0.60 k ($M_w = 602$, $M_w/M_n = 1.06$), and PEG-4.6 k ($M_w = 4621$, $M_w/M_n = 1.02$) from Sigma Chemical (St. Louis, MO). To confirm the reagent mass distribution, PEGs of 3 kDa or larger were analyzed by sodium dodecyl sulphate polyacrylamide gel electrophoresis (SDS-PAGE) in 18% gels. The discontinuous SDS-PAGE system was essentially as described for the electrophoresis of proteins (Laemmli, 1970) except that a stacking gel was omitted (Zimmerman and Murphy, 1996; Dhara and Chatterji, 1999). PEGs (20 or 100 μg) were applied to the gel and electrophoresced overnight at 50 V. Gels were stained for 1 h with Dragendorff's reagent (0.6 mM bismuth subnitrate, and 0.11 M potassium iodide in 5% (wt/vol) tartaric acid) as recommended (Dhara and Chatterji, 1999) and destained with three 5-min washes in water with shaking. All PEGs analyzed appeared as discrete bands with only slightly increased broadening with increasing M_w, in keeping with the manufacturer's M_w/M_n ratios.

Sulfhydryl-directed PEG reagents

Water-soluble, sulfhydryl-directed MePEG-OPSS (monomethoxypoly (ethylene glycol)-*o*-pyridyl disulfide) reagents were from Shearwater Polymers (Huntsville, AL). Excluding the contribution of the OPSS group (142 Da), the masses were MePEG-OPSS-0.85 k ($M_w = 848$, $M_w/M_n = 1.02$), MePEG-OPSS-1.7 k ($M_w = 1708$, $M_w/M_n = 1.02$), MePEG-OPSS-2.5 k ($M_w = 2468$, $M_w/M_n = 1.03$), and MePEG-OPSS-5.0 k ($M_w = 4988$, $M_w/M_n = 1.02$). The homogeneities of the MePEG-OPSS stocks were determined by modifying a radiolabeled, monomeric cysteine mutant of αHL, K8C, followed by separation of the products by SDS-PAGE and phosphorimager analysis (Howorka et al., 2000). PEG-modified αHL migrates more slowly than the unmodified monomeric protein in SDS gels. The mass distributions of the polymers in the MePEG-OPSS reagents were assessed from the broadening of the gel bands of MePEG-modified αHL-K8C. The bands were only slightly broadened indicating that the molecular size distribution of all four of the MePEG polymers is narrow as suggested by the M_w/M_n ratios determined by gel permeation chromatography. The pK_a value of the reactive group OPSS is 2.0, so that the molecules are uncharged at pH 8.5 (Movileanu et al., 2001).

Wild-type αHL

Heptameric wild-type αHL pores were obtained by treating αHL monomers, purified from *Staphylococcus aureus*, with deoxycholate (Bhakdi et al., 1981; Walker et al., 1992) and isolated from SDS-polyacrylamide gels as previously described (Braha et al., 1997; Cheley et al., 1999).

Cysteine mutants

The single cysteine mutants T117C and L135C were constructed by cassette mutagenesis as described previously (Cheley et al., 1999; Movileanu et al., 2001). For bilayer recordings, mutant αHL polypeptides were synthesized in vitro by coupled transcription and translation and assembled into homoheptamers by the inclusion of rabbit red blood cell membranes during synthesis as detailed earlier (Cheley et al., 1999). The gel-purified homoheptamers (~0.2 μg/ml) were stored in 50 μl aliquots at −80°C.

Planar bilayer recordings

Single-channel recordings were carried out with planar lipid membranes as described previously (Montal and Mueller, 1972; Hanke and Schlue, 1993; Movileanu et al., 2000). Both the *cis* and *trans* chambers of the apparatus contained 1 M KCl, 10 mM Tris·HCl, pH 7.5, with 100 μM EDTA, unless otherwise specified. Measurements were performed at room temperature (23 ± 0.5°C). A solvent-free planar lipid bilayer membrane of 1,2-diphytanoyl-*sn*-glycerophosphocholine (Avanti Polar Lipids, Alabaster, AL) was formed across the orifice. The transmembrane potential was applied through Ag/AgCl electrodes connected to the bath with 1.5% agar bridges (Ultra Pure DNA Grade, Bio-Rad Laboratories, Hercules, CA) containing 3 M KCl (Sigma). Protein was added to the *cis* chamber, which was at ground. A positive potential indicates a higher potential at the *trans* chamber, and a positive current is one in which cations flow from *trans* to *cis*. Single-channel currents were recorded by using a patch-clamp amplifier (Axopatch 200B, Axon Instruments, Foster City, CA) in the whole-cell mode ($\beta = 1$) with a CV-203BU headstage. The signals were low-pass filtered at 40 kHz with an 8-pole Bessel filter (Model 900, Frequency Devices, Haverhill, MA).

Data analysis and statistics

A Pentium PC equipped with a DigiData 1200 A/D converter (Axon Instruments, Foster City, CA) was used for data acquisition with Clampex 8.0 (Axon Instruments). Single-channel data for analysis were acquired at a sampling rate of 200 kHz. Acquisition of the events was carried out with the 50% threshold crossing technique. To avoid large binning promotion errors, we used a 5-μs bin width for the dwell time histograms. The promotion errors were then corrected automatically by pStat (in pClamp 8.0). The distributions of closed and open durations were fitted with sums of exponentials using the maximum likelihood method (Colquhoun and Sigworth, 1995) to estimate the most probable values of the time constants. The rise time (T_r) for the delay introduced by the filter for a single-channel transition is $T_r = 339/f_c$ μs, where f_c is the corner frequency of the filter (Colquhoun and Sigworth, 1995). In our case, $T_r = 9.2$ μs. The dead time is $T_d = 0.54T_r = 4.9$ μs, which is close to the sampling interval (5.0 μs). As the mean duration of interevent intervals is much longer than both the durations of occupancy by PEG (the short and long spikes) and the dead time, the contribution of phantom states (unoccupied-occupied compound states) to the total number of states is negligible. The time constants and the true number of events were also corrected for missed events according to a procedure similar to that developed previously (Blatz and Magleby, 1986) (see Online Supplement). The procedure was modified for a scheme with one unoccupied state (with mean duration L_0) and two occupied states (with mean durations L_1 and L_2). To calculate corrections to the rate constants, approximations were made based on the assumption $T_d < L_1, L_2 \ll L_0$. The values reported in the text are corrected unless otherwise stated. Gap-free data from the same experiments were stored simultaneously on digital audiotape at a sampling rate of 48 kHz. For display purposes, these data were filtered at 10 kHz.

In the case of recordings showing the reaction of single αHL pores with MePEG-OPSS-0.85 k, the signals were filtered at 10 kHz and sampled at 50 kHz. For the macroscopic current measurements (at least 30 channels in the bilayer), used for chemical modification experiments, the signal was filtered at a frequency of 100 Hz and sampled at 1 kHz (data not shown).

For display and further manipulation of the single-channel current or macroscopic current traces, we used pClamp 9.0 (Axon Instruments) and Origin7.0 (Microcal Software, Northampton, MA).

RESULTS

Partial blockade of the αHL pore by PEG molecules

Currents flowing through individual αHL pores (Fig. 1) were recorded at +100 mV in 1 M KCl, 10 mM Tris·HCl, pH 7.5, containing 100 μM EDTA. In the absence of PEG, the current flowing through the open (unoccupied) αHL pore was 96.3 ± 2.1 pA ($n = 32$ experiments; Figs. 2 *A* and 3 *A*). The open state was of long duration, and lasted for hours under the stated conditions. Similarly, except at extremes of pH and transmembrane potential, other authors have found that wild-type αHL pores exhibit long-lived open states (Menestrina, 1986; Korchev et al., 1995).

The addition of PEGs of various molecular masses (Fig. 1; Table 1) to the *trans* side of the bilayer, at low millimolar concentrations, produces reversible partial channel blockades. The extent of the block is very similar to the amplitude of the macroscopic current reductions produced by MePEG-OPSS reagents when they react with cysteine sulfhydryls located in the β-barrel domain (Movileanu et al., 2001). For example, four MePEG-OPSS reagents ranging from MeOPSS-PEG-0.85 k to MeOPSS-PEG-5.0 k produced a 71 ± 3% reduction in the macroscopic current after attachment of a single PEG to position 117 in the barrel in 300 mM KCl at −40 mV. The extent of block was independent of the size of the polymer (Movileanu et al., 2001). In the present work, which was conducted in 1 M KCl, PEG-2.0 k through PEG-6.0 k reduced the single-channel conductance by 67 ± 1% (Figs. 2 and 3) as determined from all-points amplitude histograms. The amplitudes were widely distributed, but this is expected given the recording procedure and the short lifetimes of the events, and the observed distributions could be simulated (www.qub.buffalo.edu) by using single-value true

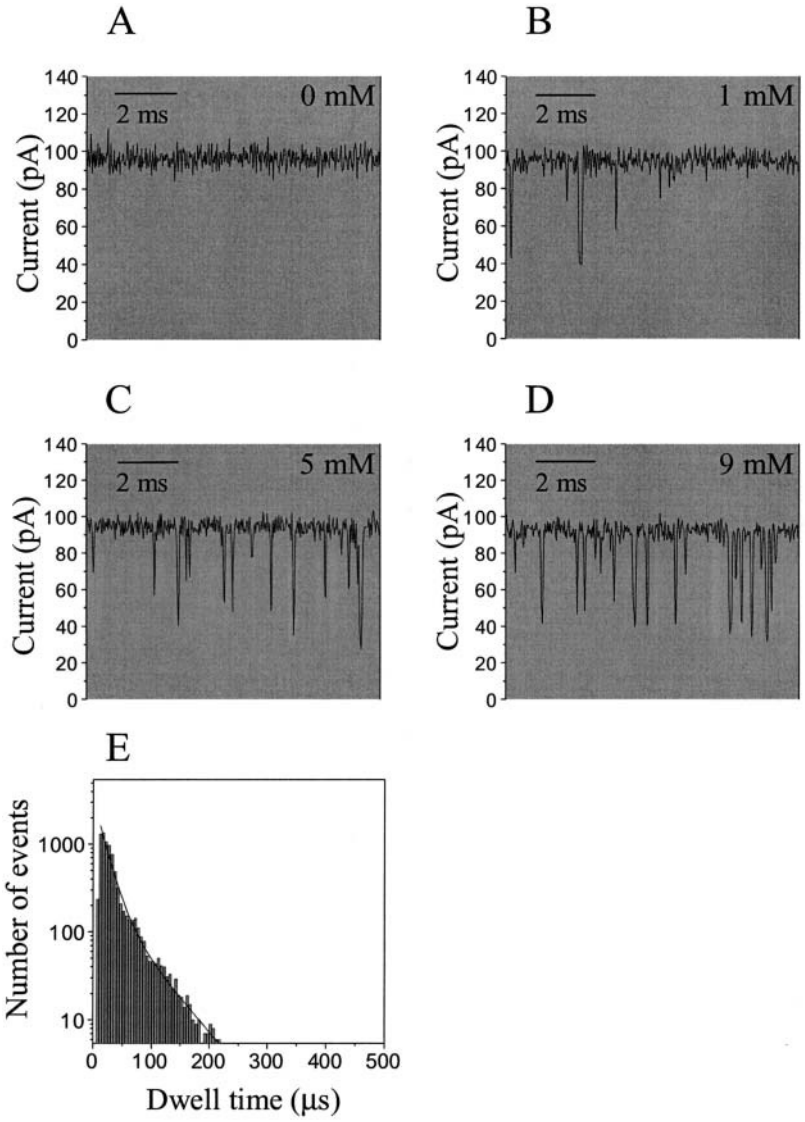

FIGURE 2 Single-channel recordings of the αHL pore in the absence and presence of PEG-0.94 k applied to the *trans* side of the bilayer. (*A*) no PEG; (*B*) 1 mM PEG-0.94 k; (*C*) 5 mM PEG-0.94 k; (*D*) 9 mM PEG-0.94 k; and (*E*) semilogarithmic dwell-time histogram for PEG occupancy events. The PEG-0.94 k concentration was 5 mM and the recording period was 10 s. The bin size is 5 μs. A double-exponential fit was made by the Marquardt-LSQ procedure. The time constants derived from this experiment, uncorrected for missed events, are 19 and 59 μs. For the traces in *A–D*, the signal, which was obtained at a transmembrane potential of +100 mV, was low-pass filtered at 10 kHz. The other conditions are in Materials and Methods. The histogram in *E* is based on a signal filtered at 40 kHz.

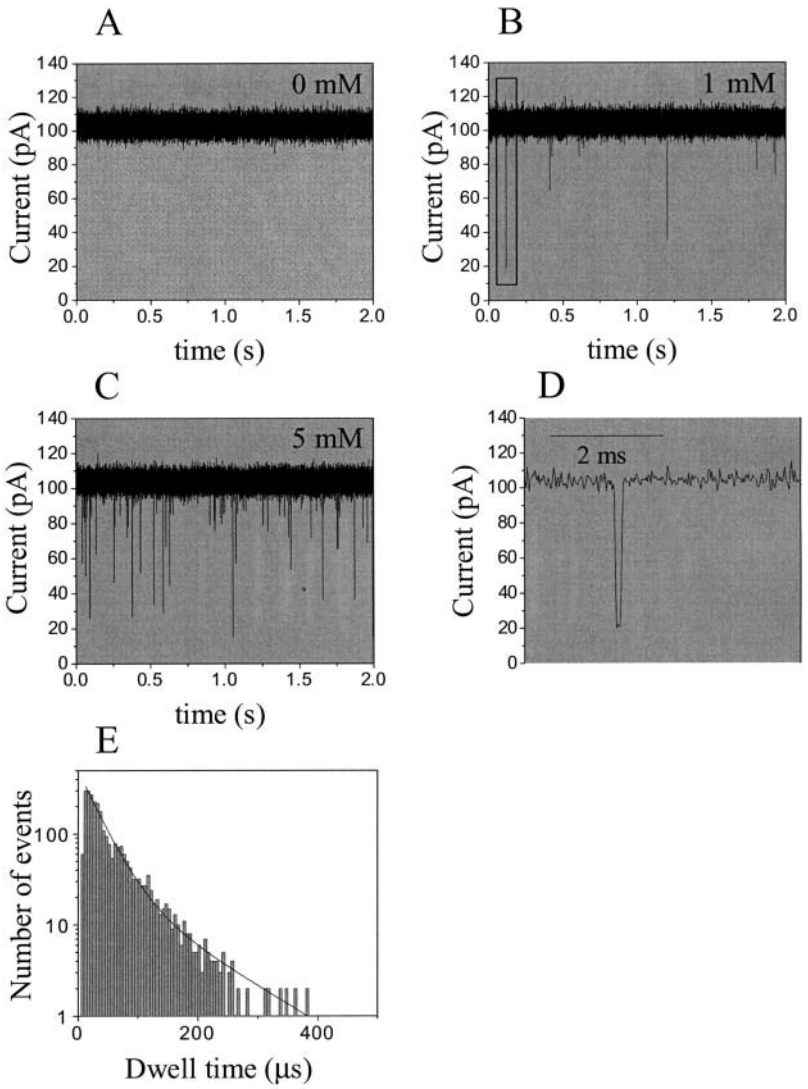

FIGURE 3 Single-channel recordings of the αHL pore in the absence and presence of PEG-6.0 k applied to the *trans* side of the bilayer: (*A*) no PEG; (*B*) 1 mM PEG-6.0 k; (*C*) 5 mM PEG-6.0 k; (*D*) expanded trace of boxed area in *B*; (*E*) semilogarithmic dwell-time histogram for PEG occupancy events. The PEG-6.0 k concentration was 5 mM and the recording period was 200 s. The bin size is 5 μs. A double exponential fit was made by the Marquardt-LSQ procedure. The derived time constants, uncorrected for missed events, are 29 and 120 μs. For the traces in *A–D*, the signal, which was obtained at a holding potential of +100 mV, was filtered at 10 kHz. The histogram in *E* is based on a signal filtered at 40 kHz.

amplitudes, two τ-values (see below), and 40-kHz filtering. The similarity between the results found with the free PEGs and those obtained by chemical modification suggests that only one PEG is located in the transmembrane β-barrel during the spikes produced by the free PEG molecules. For PEG-0.60 k and PEG-0.94 k (Fig. 2), the extents of block appeared to be lower at 45 ± 2% and 62 ± 3%, respectively. Furthermore, we found no detectable events for PEGs with a molecular mass <400 Da, most probably because the events are shorter than the rise time of the filter.

TABLE 1 Properties of the PEG polymers used in this work

M_w (kDa)	N	R_F (Å)	[*PEG*] (%)	[*PEG*]^o (%)
0.94	20	21	0.1–1.2	3.6
2.0	43	34	0.2–2.6	2.0
3.1	68	44	0.3–4.0	1.4
4.2	94	53	0.4–5.5	1.1
4.6	103	56	0.5–6.0	1.0
6.0	133	66	0.6–7.8	0.82

M_w, the weight-average molecular weight; N, the number of monomer units derived from the number-average molecular weight (M_n); R_F, the Flory radius; [*PEG*], the range of PEG concentrations used in this work expressed in % (w/v); [*PEG*]^o, the overlap concentration, which defines the gradual transition between dilute and semidilute regimes (for details, see de Gennes, 1979; Gedde, 1995).

To better understand the nature of the spikes, we measured the extent of channel block after covalent attachment of a single PEG chain within an individual αHL pore. The cysteine mutant homoheptamer $T117C_7$ was reacted with 1 mM MePEG-OPSS-0.85 k from the *trans* side of the bilayer (Fig. 4). A few seconds after addition of the reagent, without stirring, the current became decorated with short spikes (65 ± 3% block from the fully open state (level 0), $n = 4$), which most likely represent noncovalent interactions. After ~1 s, the current dropped from level 0 to level 1 (Fig. 4 *A*); the magnitude of the drop (63 ± 2%, $n = 4$) was very close to the amplitude of the blockades by free PEG-0.94 k. The shift in the current to level 1 most probably results from

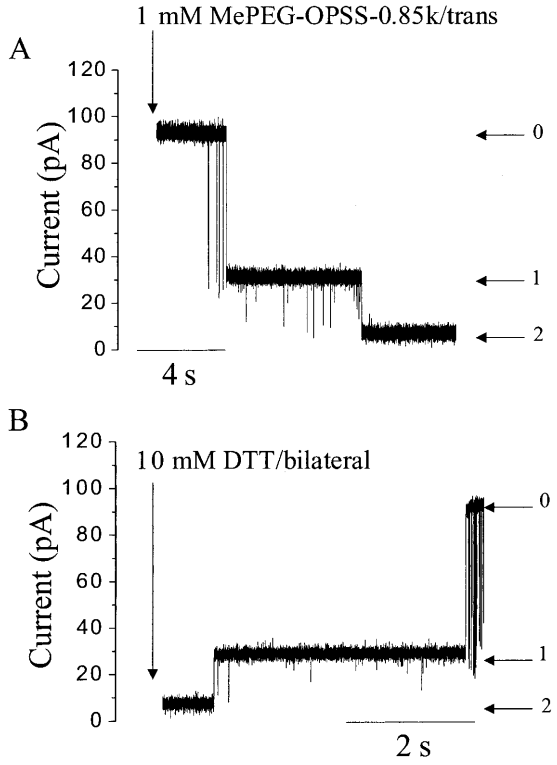

FIGURE 4 Single-channel recording with the homoheptameric cysteine mutant $T117C_7$. (*A*) MePEG-OPSS-0.85 k (1 mM) added to the *trans* chamber. The current levels are interpreted as follows: 0, fully open channel; 1, one PEG attached; 2, two PEGs attached. (*B*) Application of 10 mM DTT resulted in the cleavage of both PEG chains from the protein surface. The solution in the chambers contained 1 M KCl, 10 mM Tris·HCl, and 100 μM EDTA, pH 8.5. The signal, which was obtained at a holding potential of +100 mV, was low-pass filtered at 10 kHz.

the covalent attachment of a single MePEG-0.85 k molecule at position 117 within the lumen of the transmembrane domain of the channel.

Level 1 was also decorated with short-lived spikes, which occurred at a lower frequency than those from level 0. The spikes were still present after washing out the chambers of the apparatus, suggesting that they represent movement of the attached MePEG-0.85 k within the channel lumen. After a few seconds, a new downward shift in the single-channel current occurred to level 2 (Fig. 4 *A*), presumably as the result of a second reaction of MePEG-OPSS-0.85 k at position 117 (Fig. 4 *A*). When 10 mM DTT was added to the chambers, both PEG chains were cleaved from the Cys-117 residues as deduced from the restoration of the current to level 0 in two steps (Fig. 4 *B*).

Duration of the PEG-induced channel blocks

Semilogarithmic dwell time histograms for PEG occupancy events were fitted to two exponentials, where τ_{off-1} represents the short-duration events and τ_{off-2} the long-duration events. Typical histograms, for PEG-0.94 k and PEG-6.0 k, are shown (Figs. 2 *E* and 3 *E*, respectively). To determine the number of exponentials for the best fit, we applied the log likelihood ratio (LLR) test to compare different fitting models (McManus and Magleby, 1988; Colquhoun and Sigworth, 1995). At a confidence level of 0.95, the best model was a two-exponential fit. Fits to a three-exponential model were not significantly better as judged by the log likelihood ratio value. The two-exponential fits were significantly better than fits to stretched exponentials. The fits to the second of the two exponentials (τ_{off-2}) were distinctly better ($R = 0.97 - 1.00$, Marquardt-LSQ (least squares) procedure) than the fits to the first of the two exponentials (τ_{off-1}, $R = 0.84 - 0.88$; Figs. 2 *E* and 3 *E*).

There are several difficulties in measuring the lifetimes of events in the microsecond time domain (Blatz and Magleby, 1986; McManus et al., 1987; Colquhoun and Sigworth, 1995) and our data were corrected for binning and sampling promotion errors, and missed events. The fraction of the long events was 0.15 ± 0.05 of the total, and did not vary significantly with the PEG molecular mass. τ_{off} values were determined at seven concentrations of PEG in the range 1–13 mM. As expected, τ_{off-1} and τ_{off-2} did not vary with concentration and so the values for each PEG were averaged. τ_{off-1} shows only a slight increase from 22 ± 2 μs to 26 ± 3 μs for the range of PEGs from PEG-0.94 k to PEG-6.0 k. τ_{off-2} increases from 60 ± 7 μs to 120 ± 10 μs over the same range of PEG masses.

Dependence of the event frequency on the PEG concentration and molecular mass

By contrast with τ_{off}, the interevent intervals (τ_{on}) were strongly dependent on both PEG molecular mass and the PEG concentration in the *trans* chamber (Fig. 5). For example, at 3 mM polymer the frequencies of occurrence of the short events were PEG-0.94 k, 840 ± 60 s^{-1}; PEG-2.0 k, 180 ± 20 s^{-1}; and PEG-3.1 k, 24 ± 4 s^{-1} (Fig. 5 *A*). A similar result was obtained when the frequencies of occurrence of the long events were separated from the total (Fig. 5 *B*). For example, at 3 mM polymer the values were PEG-0.94 k, 120 ± 10 s^{-1}; PEG-2.0 k, 26 ± 2 s^{-1}; and PEG-3.1 k, 3.6 ± 0.6 s^{-1} (Fig. 5 *B*). τ_{on} values were determined for each of the two classes of events by using $\tau_{on-1} = \tau_T/f_1$ and $\tau_{on-2} = \tau_T/f_2$, where τ_T is the overall interevent interval (short and long events) and f_1 and f_2 are the number of short and long events as a fraction of the total number of events, as determined from the dwell time histograms.

Dependence of k_{on}, k_{off}, and K_f on PEG molecular mass

Rate constants for the association (k_{on}) and dissociation (k_{off}) of PEG were determined from the τ-values, by assuming a simple bimolecular interaction such that $k_{on} = 1/(\tau_{on} \cdot [PEG])$, where $[PEG]$ is the PEG concentration, and

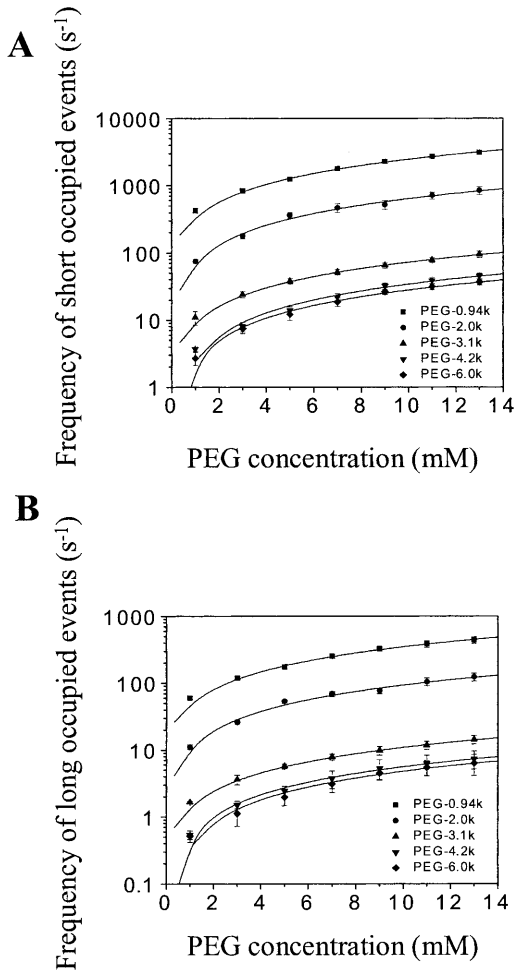

FIGURE 5 Semilogarithmic plots of the frequency of occurrence of PEG occupancy events versus PEG concentration. The values were corrected for missed events. The fits shown represent linear relationships between frequency of occurrence and PEG concentration. (*A*) Frequency of occurrence of the short occupancy events for five of the PEGs; (*B*) frequency of occurrence of the long spike events for five of the PEGs. ■, PEG-0.94 k; ●, PEG-2.0 k; ▲, PEG-3.1 k; ▼, PEG-4.2 k; ♦, PEG-6.0 k. Because $\tau_{on-1} = \tau_T/f_1$, $\tau_{on-2} = \tau_T/f_2$, and $f_1 + f_2 = 1$, the plots in *A* and *B* are related; e.g., $\tau_{on-2} = \tau_{on-1}(1/f_1-1)$.

$k_{off} = 1/\tau_{off}$ (Tables 2 and 3). k_{on} values were obtained from the slopes of plots of $1/\tau_{on}$ vs. $[PEG]$, whereas k_{off} was obtained by averaging the values obtained at the various concentrations (Fig. 6). The equilibrium association constants were then calculated for both the short and long spikes by using $K_f = k_{on}/k_{off}$ (Tables 2 and 3). At low occupancies of the pore by polymer, it can be shown that the partition coefficient $\Pi = K_f \cdot [PEG]^*$, where $[PEG]^*$ would be the molar concentration of PEG inside the pore at a fractional occupancy (F) of $F = 1$ (see Online Supplement), $[PEG]^* = 1/(N_{AV} \cdot V_{barrel})$, where N_{AV} is Avogadro's number and V_{barrel} is the internal volume of the β-barrel. Using $V_{barrel} = 10{,}000$ Å^3, $[PEG]^* = 0.17$ M. For PEGs of low molecular mass, log K_f was inversely proportional to the mass of the polymer, with a better fit for the long events (Fig. 7). At higher molecular masses, there was a cutoff above which log K_f no longer decreased (Fig. 7).

Comparison of Π-values derived from chemical modification experiments with those determined from the binding of free PEG molecules

Recently, we showed that Π-values for PEG polymers can also be determined by measuring the rates of reaction of cysteine residues in the lumen of the pore with sulfhydryl-directed PEG reagents (Movileanu et al., 2001). These values were determined by using macroscopic currents in 300 mM KCl, whereas the single-channel experiments described here were performed in 1 M KCl to reduce noise. Therefore, the chemical modification experiments were repeated for position 135 in 1 M KCl, 10 mM Tris·HCl, pH 7.5, containing 100 μM EDTA using MePEG-OPSS-0.85 k, MePEG-OPSS-1.7 k, MePEG-OPSS-2.5 k, and MePEG-OPSS-5.0 k. This is important because other workers have found that the interaction of PEG (at high concentrations) with the walls of the αHL pore is salt-concentration dependent (Bezrukov et al., 1996; Merzlyak et al., 1999). However, the values of Π obtained here in 1 M KCl were only slightly higher than those obtained in 300 mM KCl (Fig. 7; Table 4). The values of Π obtained by chemical modification are similar to those obtained for the long events from the kinetics of binding of free PEG (Fig. 7; Tables 4 and 5).

Determination of an overall partition coefficient from the total time of pore occupancy

The partition coefficients for the two classes of events (short and long) can be added to give an overall partition coefficient $\Pi_{all} = \Pi_1 + \Pi_2$. A value for Π_{all} was also obtained by using the expression

$$\Pi_{all} = \frac{1}{N_{AV} V_{barrel}} \frac{T_{occupied}}{T_{total} c_{sol}}, \quad (1)$$

where N_{AV} and V_{barrel} were defined in the previous section, and $T_{occupied}$ is the total time that the pore is occupied (short and long events) during a recording time T_{total}. It can be noted that, for low occupancy, when $\Pi = K_f \cdot [PEG]^*$ (see above), $T_{occupied}/(T_{total} c_{sol}) = K_f$.

The values obtained in this way (Table 5) were slightly lower than the values obtained from $\Pi_{all} = \Pi_1 + \Pi_2$, which arises because the use of Eq. 1 does not account for missed events.

DISCUSSION

Very little is known about the kinetics of partitioning of flexible polymer molecules into pores of nanometer dimensions, despite their fundamental importance in materials science, biotechnology, and medicine. Here, we have

TABLE 2 Kinetic constants for the short occupied states

PEG M_W	f_1 fraction of events	k_{on-1}^{exp} $(M^{-1}s^{-1}) \times 10^{-4}$	k_{on-1}^{corr} $(M^{-1}s^{-1}) \times 10^{-4}$	k_{off-1}^{exp} $(s^{-1}) \times 10^{-4}$	k_{off-1}^{corr} $(s^{-1}) \times 10^{-4}$	K_{f-1}^{exp} (M^{-1})	K_{f-1}^{corr} (M^{-1})
0.94	0.86 ± 0.05	20 ± 3	24 ± 1	4.6 ± 0.5	4.6 ± 0.5	4.3 ± 0.7	5.2 ± 0.8
2.0	0.85 ± 0.05	7.1 ± 1.9	8.7 ± 0.8	5.4 ± 0.6	5.4 ± 0.7	1.3 ± 0.2	1.6 ± 0.4
3.1	0.84 ± 0.05	0.71 ± 0.09	0.86 ± 0.11	4.4 ± 0.6	4.4 ± 0.7	0.16 ± 0.04	0.19 ± 0.04
4.2	0.84 ± 0.04	0.29 ± 0.04	0.36 ± 0.06	4.6 ± 0.5	4.6 ± 0.5	0.064 ± 0.012	0.080 ± 0.017
4.6	0.84 ± 0.05	0.28 ± 0.07	0.34 ± 0.09	4.1 ± 0.8	4.1 ± 0.8	0.065 ± 0.011	0.081 ± 0.016
6.0	0.88 ± 0.05	0.23 ± 0.04	0.28 ± 0.04	3.9 ± 0.5	4.0 ± 0.5	0.059 ± 0.010	0.069 ± 0.011

Values are the mean ± SD for at least four single-channel experiments. The PEGs were applied to the *trans* side of the bilayer. k_{on-1} is the ''on'' rate constant for the short occupied states. k_{off-1} is the ''off'' rate constant for the short occupied states. K_{f-1} is the formation constant for the short occupied states. The ''on'' rate constants were obtained from the slope of a linear fit to $1/\tau_{on}$ versus PEG concentration. The ''off'' rate constants were calculated as the reciprocal of the time constant τ_{off}, which was extracted from dwell time histograms. The superscript *exp* indicates that value was determined directly from a dwell time histogram and adjusted for promotion errors (see Materials and Methods). The superscript *corr* indicates the value was adjusted for missed events (see Online Supplement).

investigated the partitioning of PEG molecules from dilute solutions into the transmembrane β-barrels of individual protein pores formed from staphylococcal α-hemolysin. We found low values for the partition coefficients (Π) describing the distribution of PEGs between the bulk aqueous phase and the pore lumen, in keeping with a negligible interaction between the PEG chains and the interior surface of the pore. The values of Π are independent of ionic strength. For a fraction of the binding events with long dwell times, log Π decreases linearly with polymer mass in accord with the scaling law of Daoud and de Gennes describing the entry of flexible polymers into a narrow tube.

Correction for missed events

The dwell times of PEG molecules bound to the αHL pore are short and therefore it was necessary to correct for missed events. We used procedures developed earlier (Blatz and Magleby, 1986; McManus et al., 1987; Colquhoun and Sigworth, 1995), modified to accommodate a kinetic scheme in which PEG molecules form two classes of binary complexes with αHL with short and long dwell times (see Online Supplement). We compared the uncorrected and corrected data. As expected, when corrected, the dwell times for the PEGs (τ_{off}) were reduced. This effect was modest (Tables 2 and 3). The interevent intervals (τ_{on}) were also reduced when corrected. Because the missed short binding events tend to lengthen τ_{on} considerably, the effect was more appreciable (Tables 2 and 3). The overall effect of the corrections was to increase K_f by 21 ± 3%. Although this is significant, it does not, in fact, affect our interpretation of the data.

Two classes of PEG binding events

We found that there are two classes of blockades of the αHL pore by PEGs as judged by the mean durations of the events. Approximately 85% of the events are very short with dwell times that are independent of polymer mass and in the range of $\tau_{off-1} = 22$–26 μs. The long events (τ_{off-2}), which represent ~15% of the total, showed a weak dependence on polymer mass with dwell times in the range of 60 μs (PEG-0.94 k) to 120 μs (PEG-6.0 k). By contrast, the event frequency showed a dramatic dependence on polymer mass: for example, at 3 mM, PEG-0.94 k, $\tau_{on} = 1.2 \pm 0.2$ ms; and PEG-6.0 k, $\tau_{on} = 100 \pm 6$ ms. Assuming simple bimolecular interactions, the τ-values were interpreted in terms of association (k_{on}) and dissociation (k_{off}) rate constants, which were in turn used to derive formation constants (K_f) for the αHL·PEG complexes.

Molecular interpretation of the two classes of PEG binding events

The short and long binding events have several similarities. First, their amplitudes are about the same. Indeed, the

TABLE 3 Kinetic constants for the long occupied states

PEG M_W	f_2 fraction of events	k_{on-2}^{exp} $(M^{-1}s^{-1}) \times 10^{-4}$	k_{on-2}^{corr} $(M^{-1}s^{-1}) \times 10^{-4}$	k_{off-2}^{exp} $(s^{-1}) \times 10^{-4}$	k_{off-2}^{corr} $(s^{-1}) \times 10^{-4}$	K_{f-2}^{exp} (M^{-1})	K_{f-2}^{corr} (M^{-1})
0.94	0.14 ± 0.05	3.1 ± 0.3	3.8 ± 0.7	1.7 ± 0.4	1.8 ± 0.4	1.8 ± 0.4	2.1 ± 0.5
2.0	0.15 ± 0.05	1.3 ± 0.2	1.6 ± 0.2	2.0 ± 0.5	2.1 ± 0.5	0.61 ± 0.07	0.78 ± 0.16
3.1	0.16 ± 0.05	0.14 ± 0.02	0.16 ± 0.02	0.94 ± 0.25	0.96 ± 0.26	0.14 ± 0.03	0.17 ± 0.03
4.2	0.16 ± 0.05	0.061 ± 0.008	0.074 ± 0.009	0.92 ± 0.22	0.93 ± 0.23	0.066 ± 0.011	0.080 ± 0.012
4.6	0.16 ± 0.05	0.040 ± 0.011	0.047 ± 0.013	0.94 ± 0.19	0.95 ± 0.21	0.041 ± 0.008	0.050 ± 0.016
6.0	0.12 ± 0.05	0.032 ± 0.004	0.038 ± 0.004	0.84 ± 0.14	0.85 ± 0.14	0.038 ± 0.007	0.043 ± 0.006

The PEGs were applied to the *trans* side of the bilayer. k_{on-2} is the ''on'' rate constant for the long occupied states. k_{off-2} is the ''off'' rate constant for the long occupied states. K_{f-2} is the formation constant for the long occupied states. Additional details are given in Table 2.

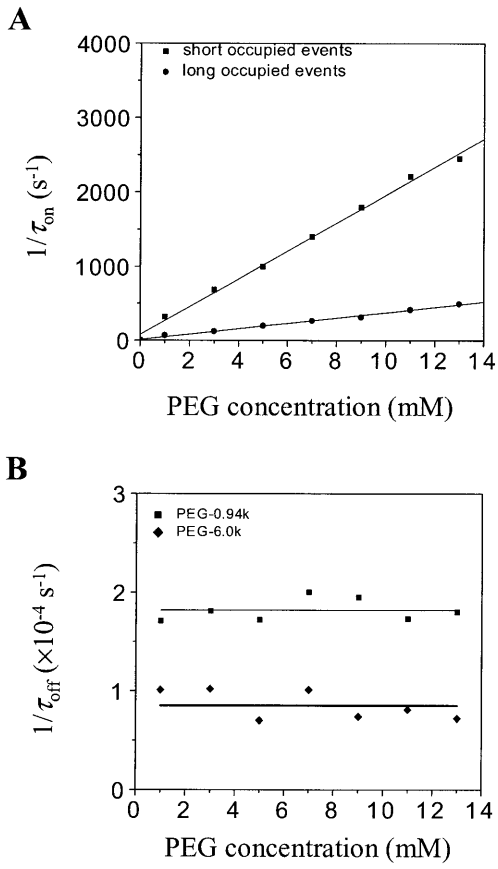

FIGURE 6 Plots of $1/\tau$ versus PEG concentration. (*A*) Plot of $1/\tau_{on}$ versus concentration for PEG-0.94 k: ■, short occupancy events; ●, long occupancy events. A representative experiment is shown. Rate constants, $k_{on} = 1/(\tau_{on} \times [PEG])$, were derived from the slopes of linear fits to such plots. (*B*) Plots of $1/\tau_{off}$ for the long events versus PEG-0.94 k (■) and PEG-6.0 k (♦) concentration. Representative experiments are shown. The dissociation rate constants, $k_{off} = 1/\tau_{off}$, are independent of PEG concentration. A similar result was found for the short events. The kinetics of PEG binding to the αHL protein pore were examined at a holding potential of +100 mV, under conditions similar to those in Figs. 2 and 3. The values of τ were adjusted to account for missed events.

amplitudes for binding events of all PEGs of >2.0 kDa are closely similar. Second, the relative preponderance of the two classes of events does not vary greatly with polymer mass. Third, the K_f values of the short and long events scale with the mass of the PEG chains in a similar (but not identical) fashion (Tables 2 and 3; Fig. 7). Finally, there is a molecular weight cutoff above which K_f no longer falls with molecular mass, again this is similar for both classes of events (Tables 2 and 3; Fig. 7). These findings suggest that the short and long events are related in molecular terms. For example, the polymer may fill the barrel as much as possible in both cases and interact with the central constriction. The event classes do differ in their τ_{off} values (by definition) and τ_{off} varies significantly with PEG mass for the long events. They also differ in their Π-values; the polymers partition somewhat more strongly into the barrel when the short events are considered (Table 5).

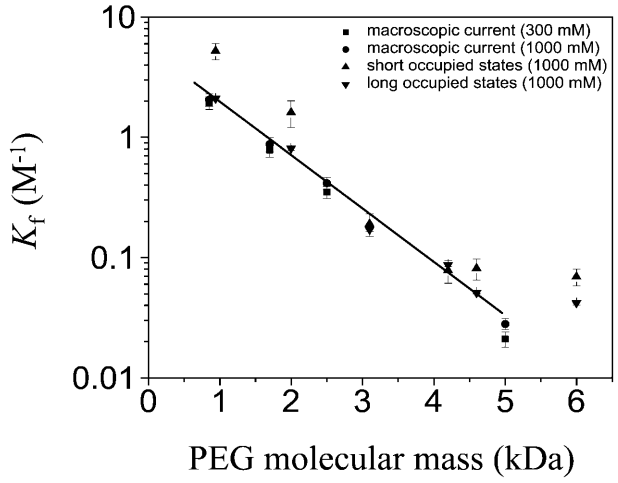

FIGURE 7 Semilogarithmic plot of the formation constant (K_f) for the αHL·PEG complex versus PEG molecular mass. ▲, mean K_f values (± SD, $n = 4$) for the short occupancy states derived from single-channel experiments to determine the kinetics of free PEG binding. ▼, mean K_f values (± SD, $n = 4$) for the long occupancy states. Values of K_f were also determined from the rates of chemical modification of $L135C_7$ with MePEG-OPSS reagents by using the scaling approach (Movileanu et al., 2001). Four experiments were performed for each molecular mass reagent: 0.85 kDa, 1.7 kDa, 2.5 kDa, and 5.0 kDa. ■, reaction carried out in 300 mM KCl (± SD, $n = 4$) (Movileanu and Bayley, 2001); ●, reaction carried out in 1000 mM KCl (± SD, $n = 4$). The line is a linear fit to the data from the chemical modification experiments carried out at 1000 mM KCl.

Therefore, the events probably differ subtly; for example, in one case the polymer may enter as a hairpin and both ends may end up near the mouth of the pore, whereas in the other case, an end may first thread into the barrel.

Partitioning of PEG molecules into the αHL pore obeys a scaling law

We previously examined the partitioning of PEG molecules into the transmembrane β-barrel of the αHL pore by determining the rates of reaction of cysteine-directed MePEG-OPSS reagents with cysteine residues located at a selection of sites within the barrel (Movileanu and Bayley, 2001). We concluded that partitioning follows the scaling law of Daoud and de Gennes (1977; de Gennes, 1979).

$$\Pi = c_{pore}/c_{solution} = \exp(-N(a/D)^{5/3}), \qquad (2)$$

where c is concentration; N, the number of repeat units in the polymer chain; a, the persistence length of the polymer; and D, the diameter of the pore. This relation applies to a narrow tube both where the Flory radius of the polymer $R_F > D$ (Daoud and de Gennes, 1977) and where $R_F \simeq D$ (de Gennes, 1979; Boyd et al., 1996). In this form, it requires that the free energy of confinement of each segment (i.e., blob) of the polymer within the pore is k_BT, where k_B is the Boltzmann constant and T the absolute temperature (Movileanu and Bayley, 2001).

TABLE 4 Partition coefficients determined from the apparent first-order rate constants for the reaction between MePEG-OPSS reagents and Cys-135 in L135C$_7$ αHL pores

MePEG-OPSS*	1000 mM KCl	300 mM KCl†
PEG-0.85k	0.34 ± 0.06	0.32 ± 0.04
PEG-1.7k	0.14 ± 0.03	0.13 ± 0.03
PEG-2.5k	0.069 ± 0.009	0.058 ± 0.008
PEG-5.0k	0.0040 ± 0.0008	0.0032 ± 0.0007

Values are the mean ± SD of four experiments. The buffer solutions also contained 10 mM Tris·HCl and 100 μM EDTA, pH 8.5. The polymer concentration in the *trans* bath was 4 mM. The applied potential was −40 mV for the experiments at 300 mM KCl and +100 mV for the experiments at 1000 mM KCl. The partition coefficients (Π) were calculated from the reaction rates by applying a scaling law, which has been shown to apply to the αHL pore (Movileanu and Bayley, 2001), $\ln k' = -N(a/D)^{5/3} + \ln k[PEG]_{sol}$, where k' is the apparent first-order reaction rate constant; a, the persistence length of the polymer (3.5 Å) (Rex et al., 1998; Kienberger et al., 2000); D, the diameter of the transmembrane barrel; k, the second-order reaction rate constant; and $[PEG]_{sol}$, the PEG concentration in the bulk aqueous phase. The slope of a plot of $\ln k'$ versus N was used to obtain $(a/D)^{5/3}$, which was used to obtain Π for the various polymers from $\Pi = ([PEG]_{\alpha HL}/[PEG]_{sol}) = \exp[-N(a/D)^{5/3}]$.
*M_n values are given for the MePEG part of the molecules only.
†These values are from Movileanu and Bayley (2001).

Values for $(a/D)^{5/3}$ were obtained from slopes of $\ln k'$ vs. N, and used to determine Π for various chain lengths of the polymer, where k' is the apparent first-order rate constant for the reaction of a MePEG-OPSS reagent within the lumen of the pore. The original measurements were performed in 300 mM KCl and are tabulated here for position 135, which is located near the midpoint of the transmembrane domain (Table 4). So that a comparison could be made with the partitioning of the free PEG molecules, the measurements were repeated for position 135 in 1 M KCl (Table 4) and the results were found to be closely similar.

The values of Π for the long binding events of free PEG molecules were closely similar to the values obtained from MePEG-OPSS modification (Fig. 7; Table 5). Therefore, these data show that a fraction of the binding events (~15%) for PEG molecules in dilute solution show the dependence on mass that would be expected from the scaling law of Daoud and de Gennes. The Π-values for the short events were somewhat larger (Fig. 7; Table 5), but of the same order of magnitude as those derived for the long events. However, the fit with the scaling law is not as good. Indeed, there is a suggestion of the sharper dependence on mass seen by Bezrukov and colleagues (Bezrukov et al., 1996; Merzlyak et al., 1999; Rostovtseva et al., 2002), but not of the extent noted in that work.

The derivation of Daoud and de Gennes requires that the polymer have no interaction with the wall of the pore and that Π decrease exponentially with polymer mass, because the partitioning of larger polymers is reduced by the unfavorable entropy of confinement. Although this approach cannot yield $\Pi > 1$, the good fit of the chemical modification data implies that the polymers do not interact strongly with the walls of the pore lumen (Movileanu and Bayley, 2001). In the measurements with the free PEG molecules, it would be possible to obtain $\Pi \gg 1$, were an interaction to occur. However, that is not the case. The highest value of Π is for PEG-0.94 k, where $\Pi_1 + \Pi_2 = 1.2$ (Table 5), and the overall Π determined from total occupancy times without correction for missed events is $\Pi_{all} = 1.1$ (Table 5). Further, by contrast with the results of Merzlyak and colleagues (Merzlyak et al., 1999), who used very high PEG concentrations, we do not find the interaction of PEG with the pore to depend on the ionic strength of the solution.

Kinetics of PEG binding to the αHL pore

For both the short and long events, k_{on} is strongly dependent upon PEG mass, although k_{off} shows only a weak dependence (Tables 2 and 3). These findings are consistent

TABLE 5 Partition coefficients (Π) of PEGs and cyclodextrins into wild-type and mutated αHL pores

Pore	PEG or CD	Π_1	Π_2	Π_{all} sum	Π_{all} measured
WT-αHL	PEG-0.94k	0.88 ± 0.12	0.36 ± 0.04	1.2	1.1 ± 0.2
WT-αHL	PEG-2.0k	0.24 ± 0.06	0.13 ± 0.02	0.37	0.29 ± 0.03
WT-αHL	PEG-3.1k	0.032 ± 0.004	0.028 ± 0.005	0.060	0.052 ± 0.006
WT-αHL	PEG-4.2k	0.012 ± 0.003	0.013 ± 0.002	0.025	0.021 ± 0.004
WT-αHL	PEG-4.6k	0.013 ± 0.003	0.0083 ± 0.0021	0.021	0.020 ± 0.003
WT-αHL	PEG-6.0k	0.011 ± 0.003	0.0072 ± 0.0014	0.018	0.017 ± 0.003
WT-αHL	βCD-1.1k	83*		n.a.	n.a.
M113N-αHL	βCD-1.1k	8.3×10^5*		n.a.	n.a.
N139Q-αHL	$s_7\beta$CD-1.7k†	6.0×10^5‡		n.a.	n.a.

Π_1 and Π_2 are the partition coefficients of the free PEGs into the lumen of the αHL pore for the short and long occupancy events, respectively, as derived from the kinetic analysis. For the cyclodextrins, the overall partition coefficient is given, calculated from K_f values as described in the text. The overall partition coefficient for the PEGs was calculated by using $\Pi_{all} = \Pi_1 + \Pi_2$ or measured directly from the uncorrected total times in occupied and unoccupied states.
*From Gu et al. (1999).
†$s_7\beta$CD is hepta-6-sulfato-βCD.
‡From Gu et al. (2001a).

with the idea that the PEG molecules are compacted in the transition state (or that there is a low preequilibrium concentration of the compact form) and that there is little interaction of the PEG with the lumenal walls of the β-barrel. Hence, k_{on} is highly dependent on PEG mass, because attainment of the transition state is entropically disfavored, although k_{off} is independent of mass because the free energy change required to reach the transition state reflects neither a loosening of the structure nor dissociation from the walls.

In our previous work on the modification of cysteine residues, we assumed that the bulk MePEG-OPSS solution is equilibrated with the solution in the β-barrel of the αHL pore. This assumption is now seen to be justified. The fastest rates of reaction of MePEG-OPSS were observed at residue 117. MeOPSS-PEG-0.85 k (4 mM) reacted with an apparent first-order rate constant of 1.2 s^{-1} and MeOPSS-PEG-5.0 k (4 mM) at 0.0072 s^{-1}. If we assume that the interactions that lead to reaction correspond to the long binding events (because the Π-values for MeOPSS-PEG and the long events are so similar), the data in Table 3 allow the rates of entry at 4 mM for PEG-0.94 k and PEG-4.6 k to be calculated as 150 s^{-1} and 1.9 s^{-1}, respectively, far faster than the rates of reaction.

The largest PEG used in the chemical modification experiment was 5.0 kDa. In the present work PEG-6.0 k was used, and in this case the Π-value was higher than predicted by the scaling law (Fig. 7). This result suggests that no more PEG can enter the pore when the polymer size exceeds ~5 kDa. As noted previously, the length of a polymer in a pore (l), arranged as a chain of blobs with $D = R_{blob}$, with an interblob distance of R_{blob}, is given by (Daoud and de Gennes, 1977):

$$l = ND^{-2/3}a^{5/3}. \quad (3)$$

When D is the internal diameter of the pore (20 Å) and a is the persistence length of PEG (3.5 Å), Eq. 3 predicts that the cutoff for a 60-Å barrel is ~2.5 kDa. Because the experimental cutoff is ~5 kDa, further elaboration of the theory to account for this deviation will be necessary.

Comparison of the binding properties of PEGs and cyclodextrins

We have also been interested in the interaction of host molecules such as cyclodextrins with the αHL pore (Gu et al., 1999, 2001a,b; Gu and Bayley, 2000) and it is constructive to compare the findings in the two areas. Although the interactions of the PEGs have been reported as partition coefficients, Π, we have reported the binding of the cyclodextrins as formation constants, K_f. For low (well below saturating) concentrations of cyclodextrin, it can be shown (see Online Supplement) that

$$\Pi = K_f[PEG]^*, \quad (4)$$

where [PEG]* is the effective concentration of a single molecule within the volume contained by the β-barrel of the αHL pore, ~0.17 M.

Using this simple relationship, we find that the Π-value for βCD and the wild-type αHL pore is 83, i.e., βCD partitions far more strongly than the smallest PEG examined, suggesting that it interacts with the lumenal wall of the transmembrane β-barrel. For several mutants of αHL, Π for βCD approaches 10^6 (Gu et al., 1999, 2001b; see also Table 5, this article). Interestingly, for one of these, the M113N homoheptamer, the interaction with PEG-2.0 k is not greatly altered (L.M., unpublished data).

Previous studies of PEG interactions with the αHL pore

Bezrukov and colleagues have investigated the interaction of PEG with αHL in detail (Bezrukov et al., 1996; Bezrukov and Kasianowicz, 1997; Merzlyak et al., 1999) and it is interesting to compare their results with ours. However, it should first be recognized that their studies were performed at very high PEG concentrations.

Bezrukov and colleagues found that the partition coefficient for transfer of PEG from bulk solution to the interior of the pore has a sharp dependence on PEG mass, which is not consistent with scaling theory, in contrast with our results (Bezrukov et al., 1996; Merzlyak et al., 1999; Rostovtseva et al., 2002). We have noted that our data for the short events do not fit the scaling prediction well and indeed show a sharper dependence on mass than the long events. However, the deviation is not of the magnitude noted in the earlier work. Further, single-channel current fluctuations in the presence of PEG suggested that PEG binds to the wall of the lumen of the pore in 1 M KCl (Bezrukov et al., 1996), whereas we have found no evidence for such an interaction. At low salt concentrations, no interaction was found (Merzlyak et al., 1999), in agreement with our observations. In addition, the Π-values quoted for αHL, a porin, and alamethicin are low (Rostovtseva et al., 2002), which is inconsistent with a strong interaction. Of course high Π-values cannot in any case be measured by using very high PEG concentrations; at 20% PEG, a Π of 5 would require 100% PEG in the pore.

Several issues make it difficult to make a direct comparison between our results and those obtained at higher PEG concentrations. In particular, the properties of PEGs in concentrated solutions change dramatically: the polymers are less hydrated and less flexible, polymer-polymer interaction is significant and the chains may behave like hard spheres, rather than highly flexible coils (de Gennes, 1979; Merzlyak et al., 1999). Another significant issue is the effect of osmotic stress on the protein under investigation (Zimmerberg and Parsegian, 1986).

It should also be noted that the existence of two classes of interaction of the αHL pore with PEGs, the short and long

events, would complicate the analysis of single channel noise, which was used in some of the earlier work. Further, both the chemical approach (Movileanu and Bayley, 2001) and the present analysis of individual polymer interactions permit Π-values to be determined accurately for polymers with molecular masses larger than 3 kDa for which $\Pi < 0.1$, which was not possible in the earlier studies.

SUMMARY

We have shown that PEG molecules partition into the αHL pore with a dependence on mass that is at least approximated by a simple scaling law. Our results also indicate that the PEGs have little interaction with the walls of the pore and that partitioning is independent of ionic strength. These findings differ from those obtained at high polymer concentrations and suggest that more experimentation and theoretical analysis will be required to understand this simple system, which is highly relevant to several more complex biological processes such as the translocation of nucleic acids and polypeptides through transmembrane pores.

SUPPLEMENTARY MATERIAL

An online supplement to this article can be found by visiting BJ Online at http://www.biophysj.org.

APPENDIX

Symbols and abbreviations

a	Persistence length of the polymer
αHL	α-hemolysin
c_{pore}	Polymer concentration inside the pore
$c_{solution}$	Polymer concentration in solution
D	Diameter of the pore
f_c	Corner frequency
F	Fractional occupancy
k_{on}	Association rate constant
k_{off}	Dissociation rate constant
K_f	Equilibrium association constant
L_0	Mean duration of unoccupied state
L_1	Mean duration of occupied state 1
L_2	Mean duration of occupied state 2
l	Length of the β-barrel
MePEG-OPSS	Methoxy-poly(ethylene glycol)-*o*-pyridyl disulfide
M_n	Number-average molecular mass
M_w	Weight-average molecular mass
N	Number of units in polymer chain
N_{AV}	Avogadro's number
PEG	Poly(ethylene glycol)
[PEG]*	Effective molar concentration of a single molecule of poly(ethylene glycol) inside the pore
Π	Partition coefficient
R_F	Flory radius
SDS-PAGE	Sodium dodecyl sulphate polyacrylamide gel electrophoresis
T_d	Dead time
$T_{occupied}$	Total time that the pore is occupied during a recording time T_{total}
T_r	Rise time
τ	Dwell time
V_{barrel}	Internal volume of the β-barrel

We thank Orit Braha, Li-Qun Gu, and Karl Magleby for valuable discussions.

This work was supported by grants from the U.S. Department of Energy, the National Institutes of Health, the Office of Naval Research (MURI-1999), and the Texas Advanced Technology Program to H.B., and the Air Force Office of Scientific Research (MURI-1998).

REFERENCES

Akeson, M., D. Branton, J. J. Kasianowicz, E. Brandin, and D. W. Deamer. 1999. Microsecond time-scale discrimination among polycytidylic acid, polyadenylic acid and polyuridylic acid as homopolymers or as segments within single RNA molecules. *Biophys. J.* 77:3227–3233.

Ambjornsson, T., S. P. Apell, Z. Konkoli, E. A. Di Marzio, and J. J. Kasianowicz. 2002. Charged polymer membrane translocation. *J. Chem. Phys.* 117:4063–4073.

Bayley, H., O. Braha, and L.-Q. Gu. 2000. Stochastic sensing with protein pores. *Adv. Matter.* 12:139–142.

Bayley, H., and P. S. Cremer. 2001. Stochastic sensors inspired by biology. *Nature.* 413:226–230.

Berezhkovskii, A. M., and I. V. Gopich. 2003. Translocation of rodlike polymers through membrane channels. *Biophys. J.* 84:787–793.

Bezrukov, S. M., and I. Vodyanoy. 1993. Probing alamethicin channels with water-soluble polymers. Effect on conductance of channel states. *Biophys. J.* 64:16–25.

Bezrukov, S. M., I. Vodyanoy, and V. A. Parsegian. 1994. Counting polymers moving through a single ion channel. *Nature.* 370:279–281.

Bezrukov, S. M., and I. Vodyanoy. 1995. Noise-induced enhancement of signal transduction across voltage-dependent ion channels. *Nature.* 378:362–364.

Bezrukov, S. M., I. Vodyanoy, R. A. Brutyan, and J. J. Kasianowicz. 1996. Dynamics and free energy of polymer partitioning into a nanoscale pore. *Macromolecules.* 29:8517–8522.

Bezrukov, S. M., and J. J. Kasianowicz. 1997. The charge state of an ion channel controls neutral polymer entry into its pore. *Eur. Biophys. J.* 26:471–476.

Bezrukov, S. M. 2000. Ion channels as molecular Coulter counters to probe metabolite transport. *J. Membr. Biol.* 174:1–13.

Bhakdi, S., R. Füssle, and J. Tranum-Jensen. 1981. Staphylococcal α-toxin: oligomerization of hydrophilic monomers to form amphiphilic hexamers induced through contact with deoxycholate micelles. *Proc. Natl. Acad. Sci. USA.* 78:5475–5479.

Bläsi, U., and R. Young. 1996. Two beginnings for a single purpose: the dual-start holins in the regulation of phage lysis. *Mol. Microbiol.* 21:675–682.

Blatz, A. L., and K. L. Magleby. 1986. Correcting single channel data for missed events. *Biophys. J.* 49:967–980.

Boyd, R. H., R. R. Chance, and G. Ver Strate. 1996. Effective dimensions of oligomers in size exclusion chromatography. A molecular dynamics simulation study. *Macromolecules.* 29:1182–1190.

Braha, O., B. Walker, S. Cheley, J. J. Kasianowicz, L. Song, J. E. Gouaux, and H. Bayley. 1997. Designed protein pores as components for biosensors. *Chem. Biol.* 4:497–505.

Carneiro, C. M. M., O. V. Krasilnikov, L. N. Yuldasheva, A. C. Campos de Carvalho, and R. A. Nogueira. 1997. Is the mammalian porin channel, VDAC, a perfect cylinder in the high conductance state? *FEBS Lett.* 416:187–189.

Cheley, S., O. Braha, X. Lu, S. Conlan, and H. Bayley. 1999. A functional protein pore with a ''retro'' transmembrane domain. *Protein Sci.* 8:1257–1267.

Cifra, P., and T. Bleha. 2001. Partition coefficients and the free energy of confinement from simulations of nonideal polymer systems. *Macromolecules.* 34:605–613.

Colquhoun, D., and F. J. Sigworth. 1995. Fitting and statistical analysis of single channel records. *In* Single-Channel Recording. Plenum Press, New York.

Daoud, M., and P.-G. de Gennes. 1977. Statistics of macromolecular solutions trapped in small pores. *J. Physique.* 38:85–93.

de Gennes, P.-G. 1979. Scaling Concepts in Polymer Physics. Cornell University Press, Ithaca, NY .

de Gennes, P.-G. 1999a. Flexible polymers in nanopores. *Adv. Polym. Sci.* 138:91–105.

de Gennes, P.-G. 1999b. Passive entry of DNA molecule into a small pore. *Proc. Natl. Acad. Sci. USA.* 96:7262–7264.

Deamer, D. W., and M. Akeson. 2000. Nanopores and nucleic acids: prospects for ultrarapid sequencing. *Trends Biotechnol.* 18:147–151.

Deamer, D. W., and D. Branton. 2002. Characterization of nucleic acids by nanopore analysis. *Acc. Chem. Res.* 35:817–825.

Dhara, D., and P. R. Chatterji. 1999. Electrophoretic transport of poly(ethylene glycol) chains through poly(acrylamide) gel. *J. Phys. Chem. B.* 103:8458–8461.

Gedde, U. W. 1995. Polymer Physics. Chapman & Hall, London, UK.

Gomis-Rüth, F. X., G. Moncalián, R. Pérez-Luque, A. González, E. Cabezón, F. de la Cruz, and M. Coll. 2001. The bacterial conjugation protein TrwB resembles ring helicases and F_1-ATPase. *Nature.* 409:637–641.

Gorbunov, A. A., and A. M. Skvortsov. 1995. Statistical properties of confined molecules. *Adv. Coll. Interf. Sci.* 62:31–108.

Gouaux, E. 1998. α-Hemolysin from *Staphylococcus aureus*: an archetype of β-barrel, channel-forming toxins. *J. Struct. Biol.* 121:110–122.

Gu, L.-Q., O. Braha, S. Conlan, S. Cheley, and H. Bayley. 1999. Stochastic sensing of organic analytes by a pore-forming protein containing a molecular adapter. *Nature.* 398:686–690.

Gu, L.-Q., and H. Bayley. 2000. Interaction of the non-covalent molecular adapter, β-cyclodextrin, with the staphylococcal α-hemolysin pore. *Biophys. J.* 79:1967–1975.

Gu, L.-Q., S. Cheley, and H. Bayley. 2001a. Capture of a single molecule in a nanocavity. *Science.* 291:636–640.

Gu, L.-Q., S. Cheley, and H. Bayley. 2001b. Prolonged residence time of a noncovalent molecular adapter, β-cyclodextrin, within the lumen of mutant α-hemolysin pores. *J. Gen. Physiol.* 118:481–494.

Hanke, W., and W.-R. Schlue. 1993. Planar Lipid Bilayers. Academic Press, London.

Henrickson, S. E., M. Misakian, B. Robertson, and J. J. Kasianowicz. 2000. Driven DNA transport into an asymmetric nanometer-scale pore. *Phys. Rev. Lett.* 85:3057–3060.

Howorka, S., L. Movileanu, X. Lu, M. Magnon, S. Cheley, O. Braha, and H. Bayley. 2000. A protein pore with a single polymer chain tethered within the lumen. *J. Am. Chem. Soc.* 122:2411–2416.

Howorka, S., L. Movileanu, O. Braha, and H. Bayley. 2001a. Kinetics of duplex formation for individual DNA strands within a single protein nanopore. *Proc. Natl. Acad. Sci. USA.* 98:12996–13001.

Howorka, S., S. Cheley, and H. Bayley. 2001b. Sequence-specific detection of individual DNA strands using engineered nanopores. *Nat. Biotechnol.* 19:636–639.

Howorka, S., and H. Bayley. 2002. Probing distance and electrical potential within a protein pore with tethered DNA. *Biophys. J.* 83:3202–3210.

Jeppesen, C., J. Y. Wong, T. L. Kuhl, J. N. Israelachvili, N. Mullah, S. Zalipsky, and C. M. Marques. 2001. Impact of polymer tether length on multiple ligand-receptor bond formation. *Science.* 293:465–468.

Johnson, A. E., and M. A. van Waes. 1999. The translocon: a dynamic gateway at the ER membrane. *Annu. Rev. Cell Dev. Biol.* 15:799–842.

Kasianowicz, J. J., E. Brandin, D. Branton, and D. W. Deamer. 1996. Characterization of individual polynucleotide molecules using a membrane channel. *Proc. Natl. Acad. Sci. USA.* 93:13770–13773.

Kasianowicz, J. J., S. E. Henrickson, H. H. Weetall, and B. Robertson. 2001. Simultaneous multianalyte detection with a nanometer-scale pore. *Analyt. Chem.* 73:2268–2272.

Kienberger, F., V. P. Pastushenko, G. Kada, H. J. Gruber, C. Riener, H. Schindler, and P. Hinterdorf. 2000. Static and dynamical properties of single poly(ethylene glycol) molecules investigated by force spectroscopy. *Single Mol.* 1:123–128.

Kong, C. Y., and M. Muthukumar. 2002. Modeling of polynucleotide translocation through proteins and nanotubes. *Electrophoresis.* 23:2697–2703.

Korchev, Y. E., G. M. Alder, A. Bakhramov, C. L. Bashford, B. S. Joomun, E. V. Sviderskaya, P. N. R. Usherwood, and C. A. Pasternak. 1995. *Staphylococcus aureus* alpha-toxin-induced pores: channel-like behavior in lipid bilayers and patch clamped cells. *J. Membr. Biol.* 143:143–151.

Krasilnikov, O. V., R. Z. Sabirov, V. I. Ternovsky, P. G. Merzliak, and J. N. Muratkhodjaev. 1992. A simple method for the determination of the pore radius of ions channels in planar lipid bilayer membranes. *FEMS Microbiol. Immunol.* 105:93–100.

Laemmli, U. K. 1970. Cleavage of structural proteins during the assembly of the head of bacteriophage T4. *Nature.* 227:680–685.

LeDuc, P., C. Haber, G. Bao, and D. Wirtz. 1999. Dynamics of individual flexible polymers in a shear flow. *Nature.* 399:564–566.

Liu, L., P. Li, and S. A. Asher. 1999. Entropic trapping of macromolecules by mesoscopic periodic voids in a polymer hydrogel. *Nature.* 397:141–144.

Lubensky, D. K., and D. R. Nelson. 1999. Driven polymer translocation through a narrow pore. *Biophys. J.* 77:1824–1838.

Madden, J. C., N. Ruiz, and M. Caparon. 2001. Cytolysin-mediated translocation (CMT): a functional equivalent of type III secretion in gram-positive bacteria. *Cell.* 104:143–152.

Marziali, A., and M. Akeson. 2001. New DNA sequencing methods. *Ann. Rev. Biomed. Eng.* 3:195–223.

McManus, O. B., A. L. Blatz, and K. L. Magleby. 1987. Sampling, log binning, fitting, and plotting durations of open and shut intervals from single channels and the effects of noise. *Pflugers Arch.* 410:530–553.

McManus, O. B., and K. L. Magleby. 1988. Kinetic states and modes of single large-conductance calcium-activated potassium channels in cultured rat skeletal muscle. *J. Physiol.* 402:79–120.

Meller, A., L. Nivon, E. Brandin, J. Golovchenko, and D. Branton. 2000. Rapid nanopore discrimination between single polynucleotide molecules. *Proc. Natl. Acad. Sci. USA.* 97:1079–1084.

Meller, A., L. Nivon, and D. Branton. 2001. Voltage-driven DNA translocations through a nanopore. *Phys. Rev. Lett.* 86:3435–3438.

Meller, A., and D. Branton. 2002. Single molecule measurements of DNA transport through a nanopore. *Electrophoresis.* 23:2583–2591.

Menestrina, G. 1986. Ionic channels formed by *Staphylococcus aureus* alpha-toxin: voltage-dependent inhibition by divalent and trivalent cations. *J. Membr. Biol.* 90:177–190.

Merzlyak, P. G., L. N. Yuldasheva, C. G. Rodrigues, C. M. M. Carneiro, O. V. Krasilnikov, and S. M. Bezrukov. 1999. Polymeric nonelectrolytes to probe pore geometry: application to the α-toxin transmembrane channel. *Biophys. J.* 77:3023–3033.

Montal, M., and P. Mueller. 1972. Formation of bimolecular membranes from lipid monolayers and study of their electrical properties. *Proc. Natl. Acad. Sci. USA.* 69:3561–3566.

Movileanu, L., S. Howorka, O. Braha, and H. Bayley. 2000. Detecting protein analytes that modulate transmembrane movement of a polymer chain within a single protein pore. *Nat. Biotechnol.* 18:1091–1095.

Movileanu, L., S. Cheley, S. Howorka, O. Braha, and H. Bayley. 2001. Location of a constriction in the lumen of a transmembrane pore by

targeted covalent attachment of polymer molecules. *J. Gen. Physiol.* 117:239–251.

Movileanu, L., and H. Bayley. 2001. Partitioning of a polymer into a nanoscopic protein pore obeys a simple scaling law. *Proc. Natl. Acad. Sci. USA.* 98:10137–10141.

Muthukumar, M. 1999. Polymer translocation through a hole. *J. Chem. Phys.* 111:10371–10374.

Muthukumar, M. 2001. Translocation of a confined polymer through a hole. *Phys. Rev. Lett.* 86:3188–3191.

Muthukumar, M. 2002. Theory of sequence effects on DNA translocation through proteins and nanopores. *Electrophoresis.* 23:1417–1420.

Nakane, J., M. Akeson, and A. Marziali. 2002. Evaluation of nanopores as candidates for electronic analyte detection. *Electrophoresis.* 23:2592–2601.

Parsegian, V. A., S. M. Bezrukov, and I. Vodyanoy. 1995. Watching small molecules move: interrogating ionic channels using neutral solutes. *Biosci. Rep.* 15:503–514.

Rex, S., M. J. Zuckermann, M. Lafleur, and J. R. Silvius. 1998. Experimental and Monte Carlo simulation studies of the thermodynamics of polyethylene glycol chains grafted to lipid bilayers. *Biophys. J.* 75: 2900–2914.

Rostovtseva, T. K., E. M. Nestorovich, and S. M. Bezrukov. 2002. Partitioning of differently sized poly(ethylene glycol)s into OmpF porin. *Biophys. J.* 82:160–169.

Salman, H., D. Zbaida, Y. Rabin, D. Chatenay, and M. Elbaum. 2001. Kinetics and mechanism of DNA uptake into the cell nucleus. *Proc. Natl. Acad. Sci. USA.* 98:7247–7252.

Slater, G. W., S. Guillouzic, M. G. Gauthier, J.-F. Mercier, M. Kenward, L. C. McCormick, and F. Tessier. 2002. Theory of DNA electrophoresis. *Electrophoresis.* 23:3791–3816.

Smith, D. E., H. P. Babcock, and S. Chu. 1999. Single-polymer dynamics in steady shear flow. *Science.* 283:1724–1727.

Song, L., M. R. Hobaugh, C. Shustak, S. Cheley, H. Bayley, and J. E. Gouaux. 1996. Structure of staphylococcal α-hemolysin, a heptameric transmembrane pore. *Science.* 274:1859–1865.

Strobl, G. 1997. The Physics of Polymers, 2nd Ed. Springer, Berlin.

Sung, W., and P. J. Park. 1996. Polymer translocation through a pore in a membrane. *Phys. Rev. Lett.* 77:783–786.

Vercoutere, W., S. Winters-Hilt, H. Olsen, D. Deamer, D. Haussler, and M. Akeson. 2001. Rapid discrimination among individual DNA hairpin molecules at single-nucleotide resolution using an ion channel. *Nat. Biotechnol.* 19:248–252.

Vercoutere, W., and M. Akeson. 2002. Biosensors for DNA sequence detection. *Curr. Opin. Chem. Biol.* 6:816–822.

Vercoutere, W. A., S. Winters-Hilt, V. S. DeGuzman, D. Deamer, S. E. Ridino, J. T. Rodgers, H. E. Olsen, A. Marziali, and M. Akeson. 2003. Discrimination among individual Watson-Crick bases pairs at the termini of single DNA hairpin molecules. *Nucleic Acids Res.* 31:1311–1318.

Vodyanoy, I., and S. M. Bezrukov. 1992. Sizing of an ion pore by access resistance measurements. *Biophys. J.* 62:10–11.

Walker, B. J., M. Krishnasastry, L. Zorn, J. J. Kasianowicz, and H. Bayley. 1992. Functional expression of the α-hemolysin of *Staphylococcus aureus* in intact *Escherichia coli* and in cell lysates. *J. Biol. Chem.* 267:10902–10909.

Wang, H., and D. Branton. 2001. Nanopores with a spark for single-molecule detection. *Nat. Biotechnol.* 19:622–623.

Winters-Hilt, S., W. Vercoutere, V. S. DeGuzman, D. Deamer, M. Akeson, and D. Haussler. 2003. Highly accurate classification of Watson-Crick basepairs on termini of single DNA molecules. *Biophys. J.* 84:967–976.

Wong, J. Y., T. L. Kuhl, J. N. Israelachvili, N. Mullah, and S. Zalipsky. 1997. Direct measurement of a tethered ligand-receptor interaction potential. *Science.* 275:820–822.

Zimmerberg, J., and V. A. Parsegian. 1986. Polymer inaccessible volume changes during opening and closing of a voltage-dependent ionic channel. *Nature.* 323:36–39.

Zimmerman, S. B., and L. D. Murphy. 1996. Electrophoresis of polyethylene glycols and related materials as sodium dodecyl sulfate complexes. *Anal. Biochem.* 234:190–193.